catalysts

MDPI

Article

A Pyrrolidine Functionalized Poly[(ethylene glycol) Methacrylate] Resin as a Heterogeneous Catalyst for Aqueous Aldol Reactions

Bert Biesemans [1], Noor Aljammal [1,2], Sambhu Radhakrishnan [3,4], Eric Breynaert [3,4], Christian V. Stevens [5], Jeroen Lauwaert [6] and Joris W. Thybaut [1,*]

1 Laboratory for Chemical Technology (LCT), Department of Materials, Textiles, and Chemical Engineering, Ghent University, Technologiepark 125, B-9052 Ghent, Belgium
2 Department of Green Chemistry and Technology, Faculty of Bioscience Engineering, Ghent University, Coupure Links 653, B-9000 Ghent, Belgium
3 NMR/X-ray Platform for Convergence Research (NMRCoRe), Katholieke Universiteit Leuven, Celestijnenlaan 200F—Box 2461, B-3001 Leuven, Belgium
4 Characterization and Application Team (COK-Kat), Center for Surface Chemistry and Catalysis, Katholieke Universiteit Leuven, Celestijnenlaan 200F—Box 2461, B-3001 Leuven, Belgium
5 SynBioC Research Group, Department of Green Chemistry and Technology, Ghent University, Coupure Links 653, B-9000 Ghent, Belgium
6 Industrial Catalysis and Adsorption Technology (INCAT), Department of Materials, Textiles, and Chemical Engineering, Ghent University, Valentin Vaerwyckweg 1, B-9000 Ghent, Belgium
* Correspondence: joris.thybaut@ugent.be; Tel.: +32-(0)-9-331-17-52

Abstract: The development of a performant aminated catalyst for aldol condensations requires the combined tuning of the active site, support and solvent system. For this purpose, a pyrrolidine group was immobilized on a swellable polymer resin. Favorable interactions between the support and water (in its role as solvent) resulted in a turnover frequency (TOF) amounting to $3.0 \pm 1.5 \times 10^{-3}$ s^{-1}, despite potential inhibition of the active sites by formation of iminium species. The affinity of the solvent for the poly[(ethylene glycol) methacrylate] support resulted in efficient swelling of the catalytic material, which was shown to be key to the observed catalytic performance.

Keywords: aldol reaction; heterogeneous catalysis; amine catalysis; polymer resin; swelling

Citation: Biesemans, B.; Aljammal, N.; Radhakrishnan, S.; Breynaert, E.; Stevens, C.V.; Lauwaert, J.; Thybaut, J.W. A Pyrrolidine Functionalized Poly[(ethylene glycol) Methacrylate] Resin as a Heterogeneous Catalyst for Aqueous Aldol Reactions. *Catalysts* **2022**, *12*, 1389. https://doi.org/10.3390/catal12111389

Academic Editor: Hugo de Lasa

Received: 3 October 2022
Accepted: 2 November 2022
Published: 8 November 2022

1. Introduction

In the past two decades, amines have gained attention as catalysts for the aldol reaction, an important carbon–carbon coupling reaction [1]. Inspired by naturally occurring enzymes, i.e., aldolase enzymes [2,3], the excellent catalytic performance of amines was first demonstrated with the amino acid proline [2,4–6]. The excellent performance of proline, offering high activity and (stereo)selectivity in the aldol condensation at relatively mild conditions for a wide range of substrates [2,7,8], preluded the promising field of organocatalysis [9]. In recognition of his pioneering work on asymmetric organocatalysis, Benjamin List was awarded the 2021 Nobel Prize in Chemistry together with David W.C. Macmillan who performed similar work on the Diels–Alder reaction [10].

List et al. [7] established that the amine group in proline acts as a Lewis base active site, catalyzing the aldol condensation via an enamine reaction mechanism [2,7], while interacting cooperatively with the adjacent carboxyl group [7,11]. Proline and proline derivatives remain, however, homogeneous catalysts, exhibiting disadvantages with respect to catalyst recovery and reusability. Therefore, more sustainable heterogeneous alternatives were investigated, in particular aminated silicas and organosilicas [1]. Several key factors determining the overall catalytic performance have, in the meantime, been identified [1].

- As active sites, primary and secondary amines provide high activity, especially in the presence of promoting groups such as hydroxyl groups [12–17].
- Additionally, the presence of (small amounts of) water was found to be favorable, both with respect to catalytic activity as well as stability [1,18,19]. In addition to these benefits, water is a widely available and environmentally benign (co-)solvent [20–22].
- In an aqueous environment, however, silica and organosilica supports exhibit poor stability as their siloxane bonds are prone to hydrolysis, causing structural degradation and leaching of active sites [1,19,23].

Several studies reported on the successful application of aminated polymers and polymer resins as aldol condensation catalysts [1,24–31]. As support material, the polymer backbone can offer sufficient tolerance against problematic degradation reactions, as such contributing to enhanced catalytic stability and reusability. In particular, a swellable polymer resin consisting of poly[(ethylene glycol) methacrylate] (abbreviated PEGMA) [32] seems to exhibit properties rendering it suitable as a catalyst support [28]. As a lightly crosslinked polymer resin (with (ethylene glycol) dimethacrylate as crosslinker), the PEGMA support can swell in a range of solvents without dissolving. Furthermore, the support offers the required thermal and chemical stability for the anticipated application [28,32]. The polymeric backbone ensures tolerance to hydrolysis, and the terminal hydroxyl groups provide options for chemical modification or fulfill a promoting role as a hydrogen bond donor. In 2020, for the first time, a stable operation in an aqueous environment at an appreciable catalytic activity was obtained with a primary amine functionalized PEGMA resin, demonstrating the feasibility of such supports for aldol reaction catalysts [28]. A PEGMA supported primary amine catalyst was demonstrated to exhibit excellent stability for at least 8 h on stream in a continuous flow setup [28].

Via computational probing of electronic as well as steric effects, De Vylder et al. [33] identified a pyrrolidine function with a potentially higher performing functionality compared to the primary amine referred to above. This cyclic secondary amine combines a high nucleophilicity with minimal steric constraints [33], and was already positively assessed as a homogeneous catalyst in aqueous aldol condensation by Singh and Chimni [34]. Immobilization of pyrrolidine on a suitable solid support, hence, brings promising perspectives for establishing a highly active heterogeneous aldol condensation catalyst. Furthermore, key determining factors of the catalytic performance such as cooperative interactions with promoting groups, or solvent and support effects [1], were not taken into account in the computational study by De Vylder et al. [33] and deserve experimental validation. Therefore, in this work, pyrrolidine groups were covalently linked to the PEGMA polymer resin. The catalytic activity of the resulting aldol reaction catalyst was assessed experimentally in an aqueous as well as a non-polar environment, taking into account solvent–support interactions.

2. Results and Discussion

2.1. Catalyst Characterization

A series of 3-(aminomethyl)pyrrolidine functionalized PEGMA resin catalysts with varying amine loadings were synthesized. After each synthesis step (see Scheme 1), the obtained material was characterized by SEM, FTIR and ^{13}C solid-state NMR.

The cross-linked poly[(ethylene glycol) methacrylate] support (PEGMA) was prepared via suspension polymerization (Scheme 1, step 1). This polymerization step yielded spherical polymer beads with a diameter ranging between 10 and 200 μm, as is visible in the SEM image of the PEGMA resin (see Figure A1, Appendix A). This is in agreement with the particle size ranges reported by Tuncel et al. (40–200 μm) [32] and De Vylder et al. (around 100 μm) [28]. The particle size distribution is provided in Figure A5, Appendix B. In the subsequent functionalization steps, SEM images indicate partial fragmentation of the PEGMA-based materials, probably due to mechanical stresses during the synthesis procedure (Figures A2–A4, Appendix A). However, as fragmentation is considered to be a mechanical process, no effect on the catalyst performance was expected.

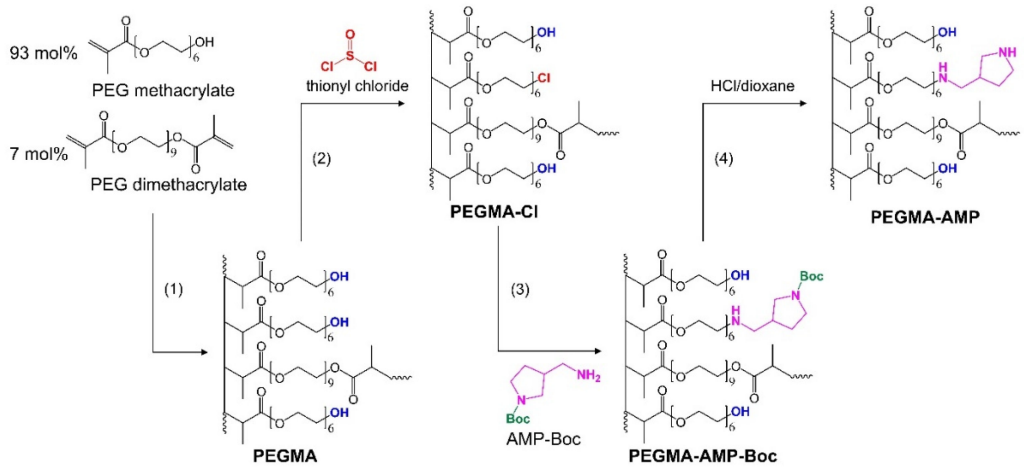

Scheme 1. The synthesis procedure of the PEGMA-AMP catalyst includes suspension polymerization of the PEGMA resin (1), introduction of Cl groups (2), substitution of Cl groups by Boc-protected pyrrolidine groups (3) and deprotection of the pyrrolidine active sites (4).

The ^{13}C NMR spectrum of the PEGMA support presented Figure 1, reveals the characteristic ^{13}C resonances associated with the ethylene glycol and the methacrylate moieties. The presence of broad resonances at 17.8, 19.7 and 45.8 ppm corresponding to the methyl groups and methylene linkages of the polymerized acrylate, confirmed the successful synthesis of the support material. This is further supported by the FTIR spectrum presented in Figure 2, as the most intense peaks correspond to the characteristic peaks of the -O-H, -C-H, -C=O and -C-O groups within the support material, appearing around 3500 cm^{-1}, 2900 cm^{-1}, 1720 cm^{-1} and 1100 cm^{-1}, respectively. However, the presence of a small fraction of non-polymerized acrylic acid terminal groups, was evidenced in the ^{13}C NMR spectrum by the presence of narrow resonances at 146 ppm and 14.8 ppm, corresponding to terminal methylene and methyl groups, respectively.

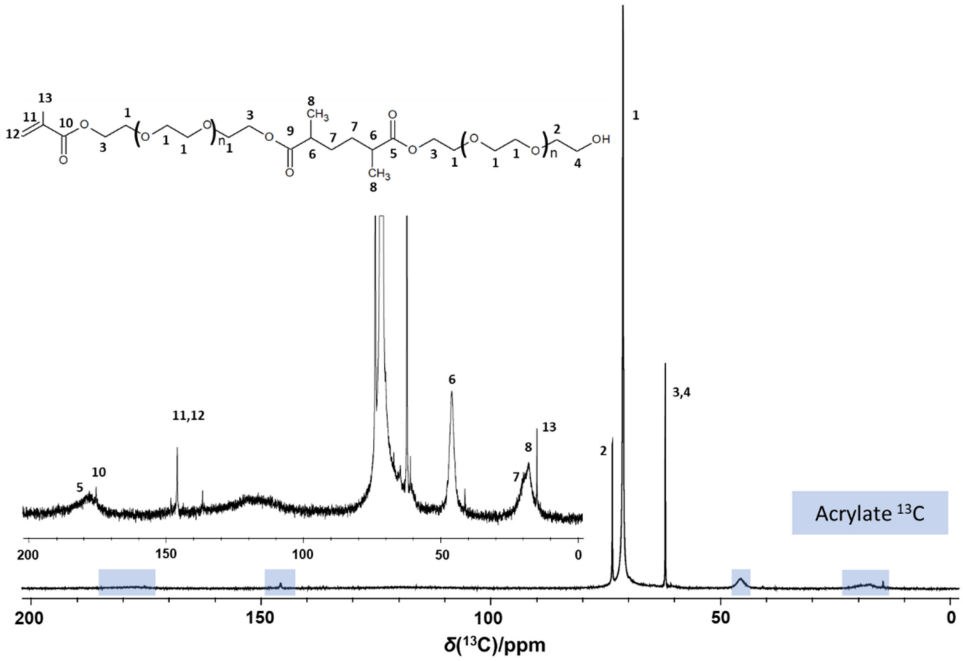

Figure 1. ^{1}H decoupled ^{13}C direct excitation solid-state NMR spectrum of the PEGMA support. Zoomed in section is given in the inset.

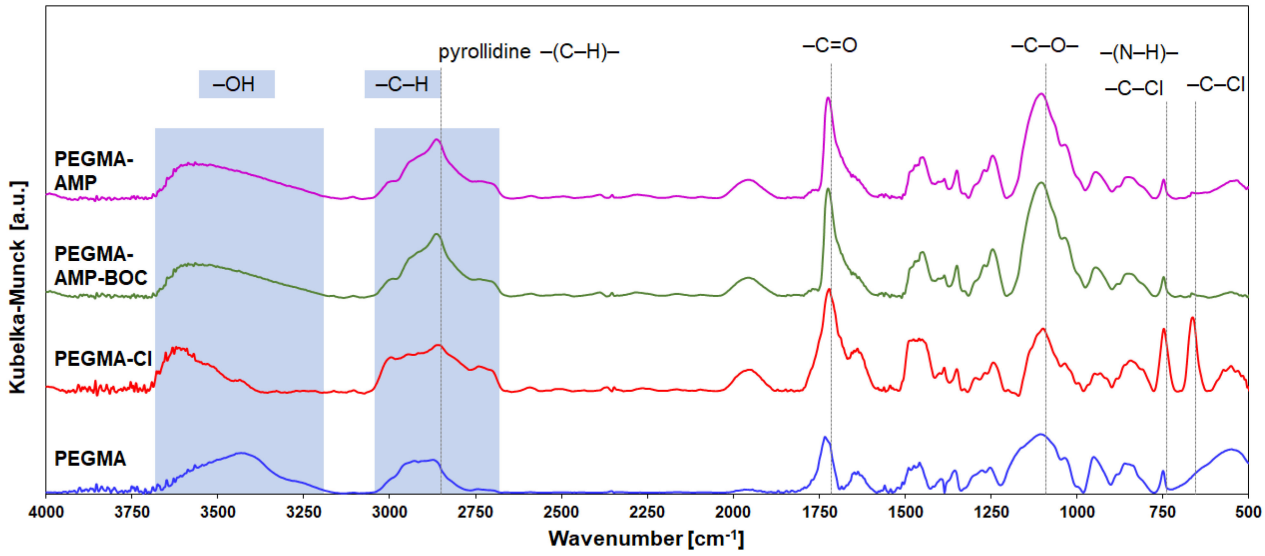

Figure 2. FTIR spectra of (from bottom to top) the PEGMA support, the chlorine-functionalized PEGMA-Cl, the protected amine-functionalized PEGMA-AMP-Boc-3 and the aminated PEGMA-AMP-3.

After the polymerization step, a partial substitution of the hydroxyl groups by Cl groups resulted in the partly chlorinated PEGMA material, denoted as PEGMA-Cl (Scheme 1, step 2). In the FTIR spectrum of the PEGMA-Cl material, a strong peak appeared at 660 cm^{-1} and the 740 cm^{-1} peak intensified, see Figure 2. Both peaks are related to the -C-Cl stretching vibration, confirming the partial substitution of hydroxyl groups by Cl-groups. Effective functionalization with Cl-groups is furthermore supported by the ^{13}C NMR spectrum (red trace, Figures 3, A6 and A7, Appendix C), by the appearance of the resonance at 44.2 ppm corresponding to the -CH_2Cl and the decrease in area of the ^{13}C peak at 62 ppm comprising the resonance of terminal -CH_2OH groups. From the elemental composition of PEGMA-Cl (see Table 1), it follows that a major fraction of hydroxyl groups (>55%) remains unsubstituted, which serve as promoting groups in the resulting catalyst [13].

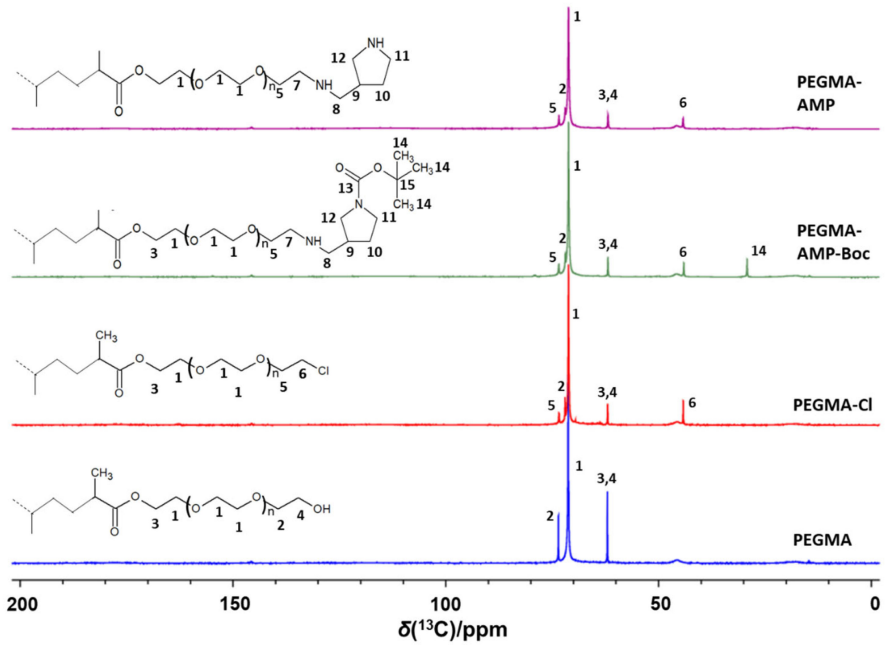

Figure 3. ^{1}H decoupled ^{13}C direct-excitation solid-state NMR spectra of (from bottom to top) the PEGMA support, the chlorine-functionalized PEGMA-Cl, the protected amine-functionalized PEGMA-AMP-Boc-3 and the aminated PEGMA-AMP-3.

Table 1. Elemental composition and amine site loading (n_{AMP}) of PEGMA, PEGMA-Cl and three batches of PEGMA-AMP (determined by CHN elemental analysis).

	PEGMA	PEGMA-Cl	PEGMA-AMP		
			1	2	3
wt% of C	53 ± 3%	53 ± 3%	56 ± 4%	57 ± 4%	57 ± 4%
wt% of H	8.6 ± 0.5%	8.4 ± 0.1%	10 ± 0.05%	9.7 ± 0.05%	9.3 ± 0.05%
wt% of O	36 ± 3%	29 ± 3%	26 ± 4%	25 ± 4%	25 ± 4%
wt% of Cl	-	7.4 ± 3%	7.1 ± 4%	6.2 ± 3%	5.7 ± 4%
wt% of N	-	-	0.2 ± 0.04%	0.54 ± 0.04%	0.8 ± 0.07%
n_{AMP} [mmol g^{-1}]	-	-	0.054 ± 0.008	0.190 ± 0.019	0.270 ± 0.014

After substitution of a part of the Cl-groups by 1-Boc-3-(aminomethyl)pyrrolidine yielding the PEGMA-AMP-Boc material (Scheme 1, step 3), the ^{13}C NMR spectrum (green trace, Figures 3, A6 and A7, Appendix C) revealed a reduction in the area of the resonance of -CH_2Cl at 44.2 ppm, and the appearance of resonances corresponding to the diamine and the protective Boc moiety, confirming successful functionalization. Only a fraction (4–24%, see Table 1) of the -CH_2Cl groups underwent functionalization, as a residual -CH_2Cl resonance was still present after functionalization. The characteristic peaks of the carbons in the pyrrolidine ring were observed at 55.5, 52.7, 50.8, 38.5 and 29.8 ppm. The intensity of the diamine resonances was, however, low due to the rather low active site loading, which according to CHN analysis, varied for three different batches between 0.054 ± 0.008 mmol·g^{-1} to 0.270 ± 0.014 mmol·g^{-1} (see Table 1). For PEGMA-AMP-3, the amine loading was validated by ^{13}C NMR as well, i.e., based on comparison of the integrated area per mass of the -CH2Cl moiety, a functionalization ratio of 24% was obtained. This agrees well with the elemental analysis data (see Table 1), showing a reduction in chloride content of 23% for PEGMA-AMP-3. The remaining hydroxyl groups on the support, may serve as promoting sites in the reaction [13]. With FTIR, the presence of amine groups could not be directly demonstrated due to the low intensity of characteristic peaks corresponding to C-N and N-H vibrations or overlap with support-related peaks. Nonetheless, an intensification at 2870 cm^{-1} was discerned (see Figure 2) corresponding to the -C-H stretching vibration within the pyrrolidine ring. Furthermore, the chlorine-related peaks at 660 cm^{-1} and 740 cm^{-1} significantly decreased, which supports the partial substitution of Cl groups by diamines.

Deprotection of the 3-(aminomethyl)pyrrolidine (AMP) groups was achieved by an acid treatment (Scheme 1, step 4), yielding the pyrrolidine functionalized resin catalyst, denoted as PEGMA-AMP. The presence of Boc groups in the PEGMA-AMP-Boc (Figure 3, green trace) sample and its removal in the PEGMA-AMP (Figure 3, purple trace) sample, was demonstrated by the respective appearance and disappearance of characteristic ^{13}C resonances of the Boc moiety around 154.7, 79.0 and 29.2 ppm (see Figures 3 and A7). CHN analysis confirmed no loss of amine groups during the Boc removal step. An upfield shift of the pyrrolidine resonances was observed upon the removal of the Boc with the electron-withdrawing carbonyl carbon group, also confirming their removal (see Figure 3). Hence, it can be concluded that the targeted 3-(aminomethyl)pyrrolidine (AMP) active sites were immobilized on the PEGMA support, even though there remains room for improving the amine substitution efficiency.

As a polymer resin, the affinity of the reaction environment, more particularly the solvent, for the PEGMA support is important for effective swelling of the resin and, hence, ensuring the accessibility to the catalytic sites inside of the resin [17]. To obtain insights into the support–solvent interactions, the swelling ratio S of the PEGMA resin, defined as the volume of the wet resin divided by that of the dry resin, was assessed in different solvents and solvent mixtures, see Table 2. The highest swelling ratio was obtained in pure water with the swollen resin roughly tripling in volume. With a volume increase of 80%, the PEGMA resin also swelled significantly in acetone. Due to the high affinity of water for the PEGMA resin, its swelling ratio in a 50/50 vol% acetone/water mixture was also very high (swelling ratio S = 2.9 ± 0.3), indicating that the resin absorbed a relatively large fraction of

water under such conditions. In *n*-hexane practically no swelling was observed due to its low affinity for the PEG-based support [35,36], while in a 50/50 vol% acetone/n-hexane mixture the material swelled only to a limited extent (S = 1.4 ± 0.3).

Table 2. Swelling ratio S of the PEGMA polymer resin determined in different solvents and solvent mixtures.

	Water	Acetone/Water (50/50 vol%)	Acetone	Acetone/N-Hexane (50/50 vol%)	*n*-Hexane
S	3.0 ± 0.3	2.9 ± 0.3	1.8 ± 0.3	1.4 ± 0.3	1.1 ± 0.2

2.2. Catalyst Performance Assessment

The catalytic activity of the PEGMA-AMP catalyst was assessed in the model aldol reaction of 4-nitrobenzaldehyde with acetone at 55 °C in an aqueous environment (50/50 vol% acetone/water) in a batch reactor. Acetone was used as an excess reagent to avoid consecutive condensation reactions of a single acetone molecule with two 4-nitrobenzaldehdyde molecules, as well as the formation of an inhibiting iminium ion from 4-nitrobenzaldehyde, which is stabilized in a polar environment, e.g., in aqueous, environment [1,18,19,37–39]. As such, acetone served both as a reagent as well as a solvent. In Figure 4, the conversion profile is presented as a function of batch time (i.e., the product of the molar amount active sites and the reaction time), allowing comparison of catalytic performance between different catalysts. A linearly increasing conversion profile was obtained, from which the turnover frequency (TOF) was determined. The main reaction product was the aldol species (see Scheme 2), formed with high selectivity, i.e., 97.7%. The secondary enone product, formed by the dehydration of the aldol product, was formed with only 2.3% selectivity. Although organocatalysts generally comply with stereoselective execution of the reaction [40], our present work focused on an optimal combination of a nucleophilic amine with minimal steric constraints, not considering stereoselectivity. The aldol and enone selectivity profiles can be found in Figure A8, Appendix D. The high aldol product selectivity could be anticipated as the two reaction products are typically in equilibrium, which in an aqueous environment is situated at the side of the aldol product [19]. The PEGMA-AMP catalyst exhibited high activity, corresponding with a TOF amounting to $3.0 \pm 1.5 \times 10^{-3}$ s^{-1}. The reaction rate furthermore remained constant, as the conversion profile increased linearly up to conversions as high as 60%, before levelling off (see Figure 4). This indicates that the rate determining step was not strongly affected by the 4-nitrobenzaldehyde concentration and that the concentration of the enamine intermediate on the catalyst surface remained fairly constant due to the excess of acetone.

As the pyrrolidine active sites are immobilized by partial substitution of hydroxyl groups, the number of promoting hydroxyl groups per active site decreases with increasing loading. Typically, it can be expected that if the ratio of promoting groups per active site becomes too low, insufficient promotion is provided, which negatively affects the catalytic activity [13,41]. However, here, similar activities were obtained for both low- and high-loaded materials, which implies that within the investigated range, the amine active sites are sufficiently promoted by the hydroxyl groups and, hence, loading effects can be excluded.

When performing the reaction with the PEGMA-Cl material or HCl, only 0.1% conversion was obtained after 3 h, compared to 6.6% with PEGMA-AMP. Hence, unsubstituted Cl-groups or amine salts with chlorine that remain on the PEGMA-AMP catalyst are not expected to contribute significantly to its (high) activity. Note that De Vylder et al. [28] have already demonstrated that the amine group serving as an anchoring point for the pyrrolidine group is not catalytically active, due to excessive steric hinderance [28]. Hence, only the secondary amine within the pyrrolidine group is considered to be catalytically active.

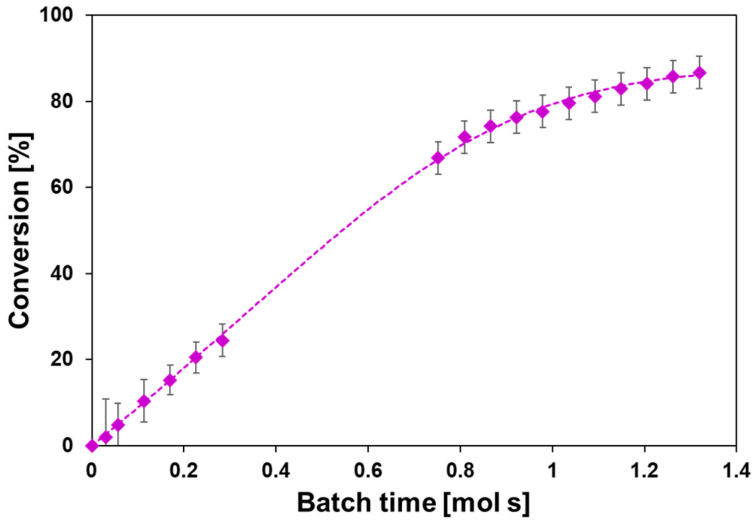

Figure 4. Conversion profile as a function of batch time (molar amount active sites x time) for the PEGMA-AMP-3 catalyst in the aldol condensation of 4-nitrobenzaldehyde with acetone at 55 °C in a 50/50 vol% mixture of acetone/water. Error bars represent the 95% confidence interval. Line is a guide for the eye.

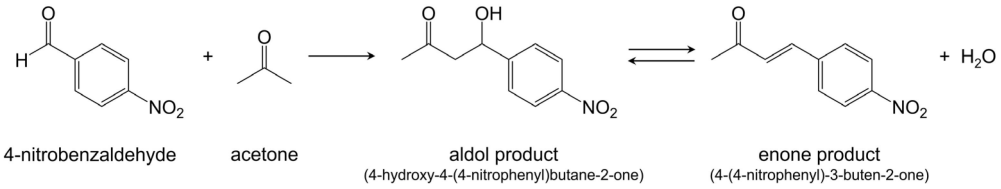

Scheme 2. Model aldol reaction of 4-nitrobenzaldehyde with acetone, yielding the aldol product (4-hydroxy-4-(4-nitrophenyl)butan-2-one), which can, subsequently, dehydrate to the enone product (4-(4-nitrophenyl)-3-buten-2-one).

As the investigated reaction of 4-nitrobenzaldehyde with acetone is a widely adopted model reaction in aldol condensation research, it is possible to compare the performance of PEGMA-AMP to that of other catalysts for which activity data are available, see Table 3. A comparison to proline-based catalysts is not feasible due to the lack of relevant activity data. Nonetheless, proline is generally considered to perform poorly in aqueous environment [8,42,43], although there are indications that supplementing the reaction environment with smaller amounts of water can lead to optimization [8,43–46]. In comparison to a PEGMA-supported methyl-substituted secondary amine tested under identical conditions by De Vylder et al. [28], PEGMA-AMP exhibited a 10 times higher activity (see Table 3, entry 1–2). To a certain extent, this improvement could be due to the higher base strength of the pyrrolidine site ($pK_a > 11$) [47] as compared to the methyl-substituted secondary amine site ($pK_a \approx 10$) [47]. After all, amines, in their role of nucleophilic sites, activate the carbonyl compound by engaging in a reversible bond [9]. However, steric effects should not be excluded as they are known to significantly affect the catalyst performance, even with relatively small substituents [11,14,15,33]. For the AMP site, steric hindrance is minimized due to the pyrrolidine structure, while the methyl substituent of the other secondary amine constitutes a small, though non-negligible burden [33].

Table 3. Overview of batch screening conditions and obtained turnover frequencies (TOF) exhibited by the PEGMA-AMP catalyst, compared to PEGMA-supported methyl-substituted secondary and primary amines as reported by De Vylder et al. [28], and a silica-supported methyl-substituted secondary amine as reported by Lauwaert et al. [15]. The solvent is applied in a 50/50 vol% mixture with acetone.

Entry	Catalyst	T [°C]	Solvent	TOF [s^{-1}]
1	PEGMA-supported pyrrolidine (PEGMA-AMP)	55	water	$3.0 \pm 1.5 \times 10^{-3}$
2	PEGMA-supported Me-substituted secondary amine [28]	55	water	$0.31 \pm 0.02 \times 10^{-3}$
3	PEGMA-supported primary amine [28]	55	water	$0.63 \pm 0.04 \times 10^{-3}$
4	PEGMA-supported pyrrolidine (PEGMA-AMP)	55	*n*-hexane	$0.006 \pm 0.0001 \times 10^{-3}$
5	Silica-supported Me-substituted secondary amine [15]	45	*n*-hexane	$3.30 \pm 0.15 \times 10^{-3}$

Strikingly, the PEGMA-AMP catalyst also provided a five-fold increase in activity compared to a PEGMA-supported primary amine, tested under identical conditions by De Vylder et al. [28], see Table 3, entry 3. In aqueous environment, the activity of secondary amines is generally inhibited by formation of an iminium ion, i.e., a charged species that is stabilized by the polar protic solvent [1,13,18]. Conversely, the activity of primary amines is not impaired in aqueous environments, as the analogous, inhibiting species on primary amines is a neutral imine that is not stabilized in polar protic solvents [1,18,37]. Moreover, swelling experiments indicated that the PEGMA support had a higher affinity for water than for acetone (see above). A high affinity of the support for specific species in the reaction mixture has already been demonstrated to lead to local enrichment of this species inside the catalyst, creating a local environment that is different from the bulk aqueous solution, which in turn may affect the catalyst performance [30,38,48–50]. The relatively high swelling ratio in a 50/50 vol% acetone/water mixture (see above) suggests that in the reaction environment, PEGMA-supported catalysts will be enriched with water and the amine active sites are exposed to a more pronouncedly polar environment. Even under these conditions, the PEGMA-AMP catalyst exhibited a high activity with a TOF of $3.0 \pm 1.5 \times 10^{-3}$ s^{-1}, which suggests that the intrinsic activity of the AMP site, i.e., in the absence of inhibition, might be even higher.

In a nonpolar environment, such inhibition phenomena are suppressed, which could potentially enhance the catalytic performance. It would therefore be advantageous to apply the PEGMA-AMP catalyst in a non-polar solvent. In a 50/50 vol% acetone/*n*-hexane mixture, however, PEGMA-AMP provided very low activity with a TOF amounting to only $6.0 \pm 1.1 \times 10^{-6}$ s^{-1}, which is a factor 500 lower than in the aqueous environment. Given the low swelling ratio of the PEGMA support in *n*-hexane (see above), the poor catalytic activity is predominantly related to the poor swelling behavior of the catalyst in the acetone/*n*-hexane mixture. Secondary amines, which are not subjected to extensive steric hindrance, have already been demonstrated to exhibit high activities in a non-polar environment; e.g., the best performing aminated aldol reaction catalyst reported in the literature, methyl-substituted secondary amine on silica, was tested under similar conditions (albeit at a lower temperature) [15], see Table 3, entry 5. A poor swelling behavior, however, compromises both the accessibility of the amine sites [17], as well as interactions between neighboring active and promoting sites [51,52]. The current PEGMA support had a higher affinity for polar solvents, such as water and acetone, while being virtually incompatible with nonpolar solvents, such as *n*-hexane [35,36]. Improvement of the catalytic performance could, hence, be obtained by further tuning of the support properties or selection of a compatible nonpolar solvent, such that effective swelling is guaranteed.

3. Materials and Methods

3.1. Catalyst Synthesis

Cross-linked poly[(ethylene glycol) methacrylate] (PEGMA) was prepared via suspension polymerization (Scheme 1, step 1), following the procedure of Tuncel et al. [32]. In a 100 mL one-neck round-bottom flask with a reflux cooler and a 2.5 cm magnetic stirring bar, the continuous phase was prepared, consisting of 80 mL double deionized water and 400 mg polyvinylpyrrolidone (K30, MW 40000, Sigma-Aldrich, Shanghai, China). The dispersed phase consisted of a mixture of 11 mL cyclohexanol (ReagentPlus®, 99%, Sigma-Aldrich, China), 4.0 mL 1-octanol (for synthesis, ≥99%, Sigma-Aldrich, Darmstadt, Germany), 8.0 mL hexaethylene glycol methacrylate macromonomer (Mn = 360, Sigma-Aldrich, St. Louis, MO, USA), and 1.2 mL nonaethylene glycol dimethacrylate macromonomer (Mn = 750, Sigma-Aldrich, USA). 1 min after adding 0.24 g of initiator, benzoyl peroxide (Luperox® A98, reagent grade, ≥98%, Sigma-Aldrich, USA), to the dispersed phase, the latter solution was added to the continuous phase. The reaction mixture was stirred for 4 h at 85 °C and 700 rpm and 1 h at 95 °C and 700 rpm. Afterwards, the polymerized resin beads were filtered off over a glass filter (Por 4), washed twice in acetone (99%, Acros organics, Madrid, Spain) and dried overnight under vacuum at 50 °C.

Subsequently, a part of the hydroxyl end groups was substituted by Cl groups (PEGMA-Cl, Scheme 1, step 2), following the procedure of De Vylder et al. [28]. The material was added to a solution of 80 mL dry toluene (ROTIDRY®Sept, ≥99.5%, ≤30 ppm H_2O, Carl Roth, Karlsruhe, Germany), 0.66 mL pyridine (ReagentPlus®, ≥99%, Sigma-Aldrich, Gillingham, UK), and 0.6 mL thionyl chloride (ReagentPlus®, ≥99%, Sigma-Aldrich, Steinheim, Germany) in a 100 mL one-neck round-bottom flask with a reflux cooler and a 2.5 cm magnetic stirring bar. The mixture was stirred for 4 h at 75 °C and 450 rpm. Afterwards, the material was filtered over a glass filter (Por 4), and washed twice in dry ethanol (100% v.p., Chem-Lab, Zedelgem, Belgium).

Afterwards, the Cl groups of PEGMA-Cl were substituted by Boc-protected amine groups (Scheme 1, step 3). Therefore, PEGMA-Cl was added to a solution of 80 mL dry toluene (ROTIDRY®Sept, ≥99.5%, ≤30 ppm H_2O, Carl Roth, Germany), 3.72 mL *N*,*N*-diisopropylethylamine (ReagentPlus®, ≥99%, Sigma-Aldrich, Germany) and the amine precursor, 1-Boc-3-(aminomethyl)pyrrolidine (AMP-Boc, ≥94%, racemate, Sigma-Aldrich, China), in a 100 mL one-neck round-bottom flask with a reflux cooler and a 2.5 cm magnetic stirring bar. The amount of amine precursor was varied between 1.5, 3.6 and 4.0 g of precursor, to obtain different amine loadings (resulting in batches 1, 2 and 3, see also Table 1). The mixture was refluxed for 48 h at 110 °C and 450 rpm. Afterwards, the material was filtered over a glass filter (Por 4), and washed twice in dry ethanol (100% v.p., Chem-Lab, Belgium). These materials are denoted as PEGMA-AMP-Boc.

Finally, the Boc-protecting groups were removed by washing for 2 h in 80 mL of a concentrated HCl solution (4 M HCl in dioxane, Sigma Aldrich, Germany) [53,54] (Scheme 1, step 4). After filtering over a glass filter (Por 4), and washing twice in a large excess of dry ethanol, the material was dried overnight under vacuum at 50 °C, resulting in the final catalyst, denoted as PEGMA-AMP.

3.2. Catalyst Characterization

Scanning electron microscopy (SEM) was performed on a SEM JEOL JSM 5400 (JEOL Europe B.V., Zaventem, Belgium) at 20 kV and was used to verify the structure of the polymer particles and assess the particle size range. Polymer samples were spread on carbon tape and sputter coated with a layer of gold (<5 nm) in order to avoid charge build-up. The size of approximately 100 polymer beads was determined on 6 SEM micrographs for determining a particle size distribution.

Further validation of the synthesis procedure was performed by means of Fourier transform infrared (FTIR) spectroscopy and solid-state ^{13}C NMR. To ensure sufficient resolution, the material with the highest loading of functional groups was used. FTIR was performed on a Brüker Tensor 27 with an MCT detector (Brüker Optik GmbH, Ettlingen, Germany).

Measurements were performed in transmission mode at wavelengths between 400 cm^{-1} and 4000 cm^{-1} for PEGMA, PEGMA-Cl, PEGMA-AMP-Boc-3 and PEGMA-AMP-3. The samples were prepared as a sandwich structure in a mixture with KBr.

Solid-state ^{13}C MAS NMR was performed on a Bruker 800 MHz Avance Neo spectrometer (Bruker Belgium NV, Kontich, Belgium) equipped with a $^{1}H/^{2}H/^{13}C/^{15}N$ high-resolution magic angle spinning probe. The samples were packed in a 4 mm ZrO_2 rotor and spun at 15 kHz MAS speed. ^{1}H decoupled ^{13}C NMR spectra (Waltz64 decoupling) were acquired with a $\pi/2$ pulse at 20 kHz RF strength and a recycle delay of 40 s. 512 transients were recorded for PEGMA, PEGMA-Cl and 4480 transients for PEGMA-AMP-Boc-3 and PEGMA-AMP-3.

The amine site loading and the C, H and N mass percentage were determined by elemental (CHN) analysis. The measurements were performed on a Thermo Scientific Flash 2000 Series elemental analyzer (Interscience, Ottignies-Louvain-la-Neuve, Belgium) using V_2O_5 as catalyst. O and Cl mass percentages were derived from the C, H and N mass percentages assuming a closing mass balance.

For PEGMA-AMP-3, the amine loading was also validated by the ^{13}C-SS-NMR spectra. The solid-state NMR spectra were acquired for PEGMA-AMP-3 obeying a quantitative methodology [55,56] (the same coil filling factor, similar Q-factor and optimized relaxation delays). The quantification of -CH_2Cl moieties remaining after AMP functionalization relative to the PEGMA-Cl was performed via spectral decomposition using DMFIT software [57].

The swelling ratio of the resin in the presence of a solvent was determined as the volume of the wet resin divided by that of the dry resin. Therefore, about 300 mg of the material was submersed in either 10 mL of a pure solvent or 10 mL of a solvent mixture, and allowed to swell for 60 min. As a solvent, either water (18.20 MΩ cm double deionized), acetone (99.6%, Acros organics, Spain) or *n*-hexane (99%, Chem-lab, Belgium) were used. The swollen material was filtered off over filter paper (MN 640 d). Subsequently, the wet resin was dried at 60 °C until no further mass loss was observed, i.e., for at least 24 h, and the volume of the absorbed solvent (V_s) was derived from the mass difference before and after drying. The swelling ratio S was then determined according to Equation (1). Based on repeat experiments, the error on the measurements was determined as 1.96 times the standard deviation, corresponding to the 95% confidence interval.

$$S = \frac{V_s}{V_d} \quad (1)$$

where V_s is the volume of the swollen resin and V_d the volume of the dry resin.

3.3. Catalyst Performance Assessment

The catalytic activity was evaluated in the aldol reaction of 4-nitrobenzaldehyde (99%, Acros organics, Shanghai, China) with acetone (99.6%, Acros organics, Spain). The reaction was performed in a batch-type reactor (Parr® 4560 mini batch reactor, 300 mL, Parr Instrument Company, Moline, IL, USA) at 55 °C and stirring speed ±300 rpm, with 0.45 g 4-nitrobenzadehyde, 45 g acetone and a solvent, either 55 g water (18.20 MΩ cm double deionized) or 38 g *n*-hexane (99%, Chem-lab, Belgium). 0.25 g methyl-4-nitrobenzoate (≥99%, Sigma Aldrich, United Kingdom) was used as internal standard. For catalytic tests, 0.15 g of PEGMA-AMP was added to the reactor. The effect of the remaining Cl groups was assessed by adding either 0.26 g of PEGMA-Cl or 0.2 mL of a 4 M HCl/dioxane solution to the reactor. The reaction was monitored for 3 h by taking 8 samples (300 µL) of the reaction mixture which were analyzed by liquid chromatography performed on an Agilent 1100 reversed-phase high-performance liquid chromatography (HPLC, Agilent Technologies, Santa Clara, CA, USA). The catalyst activity was assessed by the turnover frequency (TOF), determined from the slope of the initial conversion, corresponding to differential conditions, as a function of the batch time. The latter was defined as the product of two main variables governing the reaction, namely the reaction time and the number of amine active sites

present in the reactor. Repeat experiments were performed to determine the error of the measurements defined as the 95% confidence interval (1.96 times the standard deviation).

4. Conclusions & Perspectives

A poly[(ethylene glycol) methacrylate] (PEGMA) resin was successfully functionalized with 3-(aminomethyl)pyrrolidine (AMP). The resulting PEGMA-AMP catalyst was demonstrated to exhibit high activity in the model aldol reaction of 4-nitrobenzaldehyde with acetone at 55 °C in a 50/50 vol% mixture of acetone/water, attaining an average TOF of $3.0 \pm 1.5 \cdot 10^{-3}$ s^{-1}. The adequate performance of the catalyst is attributed to the selection of an amine active site with both high alkalinity and minimal steric hindrance, coupled to a swellable polymer resin support comprising promoting groups. Applying the catalyst in a nonpolar environment, which would enhance the stability of the pyrrolidine active site, resulted in a low catalytic activity, due to a poor swelling of the PEGMA support. Hence, further tuning of the support as a function of the solvent used may enhance the catalyst's performance. In addition, applying other substrates and ketones, while also taking into account the enrichment and swelling effects, could broaden the scope of the catalyst.

Author Contributions: Conceptualization, B.B., J.L. and J.W.T.; methodology, B.B., J.L., S.R. and E.B.; formal analysis, B.B., S.R., E.B. and C.V.S.; investigation, B.B., N.A., S.R., E.B. and C.V.S.; resources, E.B., C.V.S. and J.W.T.; data curation, B.B., S.R. and E.B.; writing—original draft preparation, B.B.; writing—review and editing, J.L., S.R., E.B. and J.W.T.; visualization, B.B., S.R. and E.B.; supervision, J.L. and J.W.T.; project administration, J.W.T.; funding acquisition, B.B., E.B., C.V.S., J.L. and J.W.T. All authors have read and agreed to the published version of the manuscript.

Funding: This work was supported by the Special Research Fund (BOF) of Ghent University through Grant Number 01D33318. J.L. acknowledges the Research Foundation—Flanders (FWO) for financial support (Grant Number 12Z2221 N). NMRCoRe is supported by the Hercules Foundation (AKUL/13/21), by the Flemish Government as an international research infrastructure (I001321N—Nuclear Magnetic Resonance Spectroscopy Platform for Molecular Water Research) and by department EWI via the Hermes Fund (AH.2016.134). E.B. and S.R. acknowledge funding from the European Research Council (ERC) under the European Union's Horizon 2020 research and innovation program under grant agreement No. 834134 (WATUSO). This work was partially supported by Department of Economy, Science and Innovation of the Flemish Government (EWI, VV023/07).

Data Availability Statement: The data presented in this study are openly available in Zenodo and/or Harvard dataverse.

Acknowledgments: The authors would like to thank Parviz Yazdani and Zinat Zanganeh for their help with the FTIR measurements, Andreas Eschenbacher and Marvin Kusenberg for their help with the (CHN) elemental analysis, Maarten Claes for performing additional analyses and Hilde Poelman, Wim Rogiers and Lambert Peka Tchokam for their practical support.

Conflicts of Interest: The authors declare no conflict of interest.

Appendix A. SEM Images

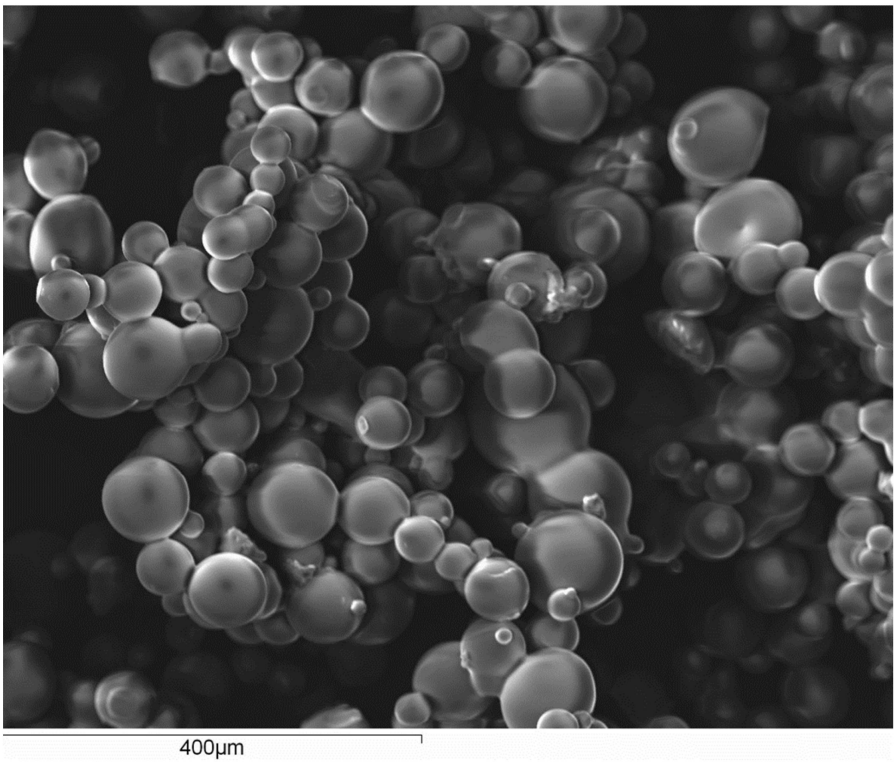

Figure A1. SEM image of PEGMA polymer resin (magnification ×150).

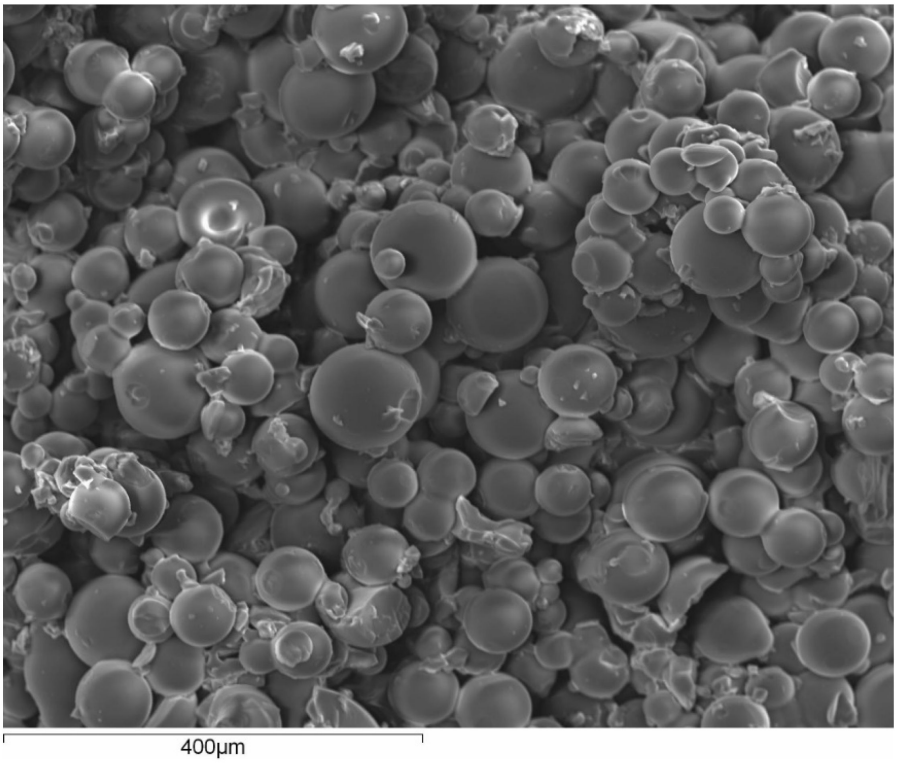

Figure A2. SEM image of PEGMA-Cl (magnification ×150).

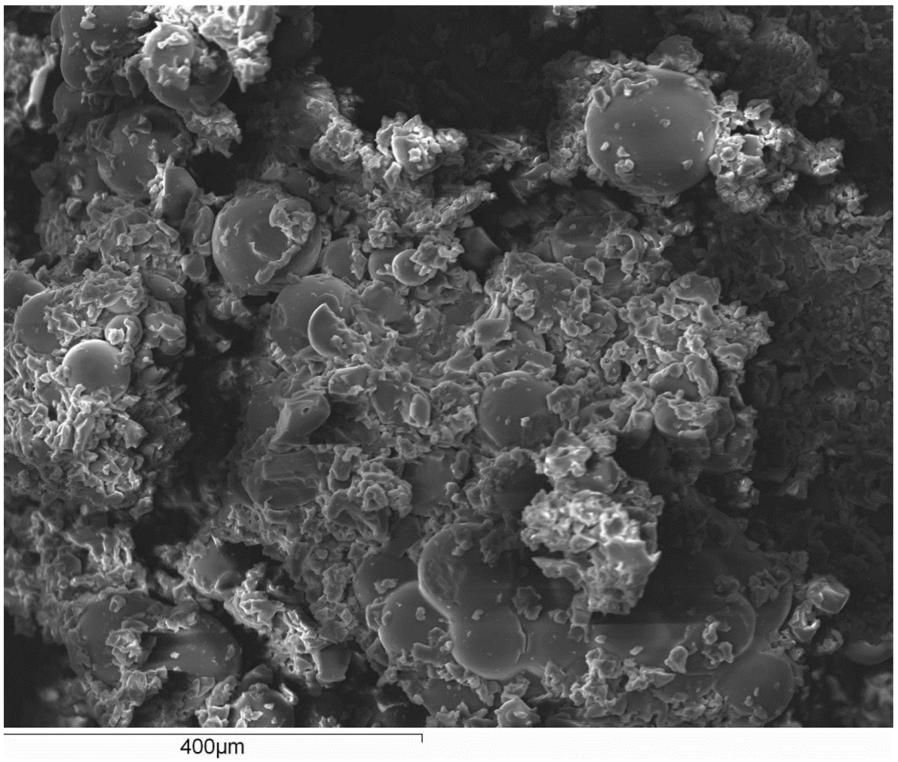

Figure A3. SEM image of PEGMA-AMP-Boc-3 (magnification ×150).

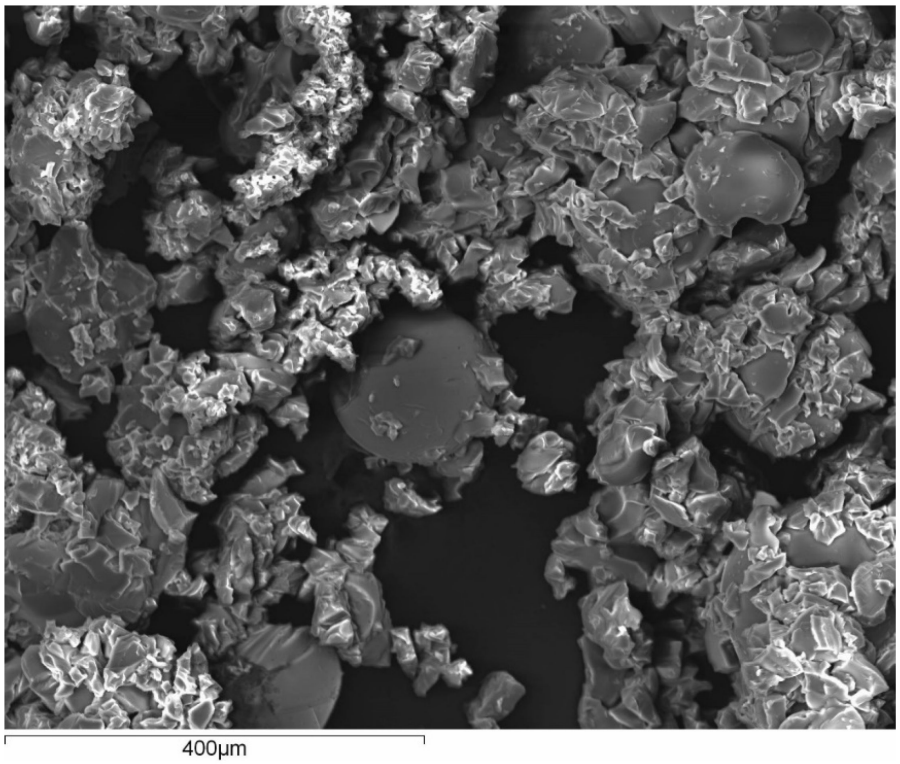

Figure A4. SEM image of PEGMA-AMP-3 (magnification ×150).

Appendix B. Particle Size Distribution

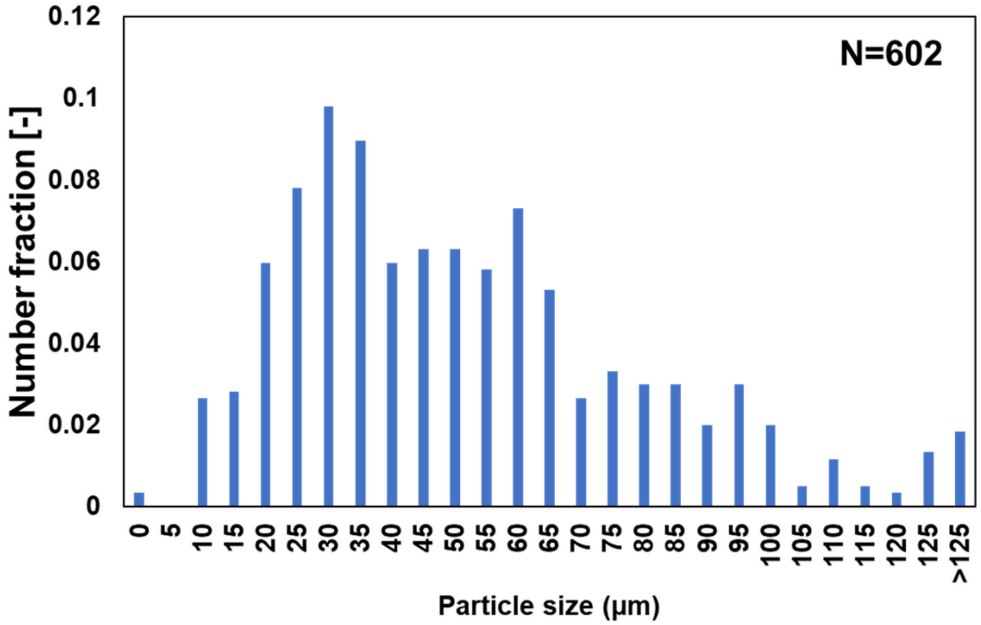

Figure A5. Particle size distribution of PEGMA gel beads.

Appendix C. Additional ^{13}C NMR Spectra

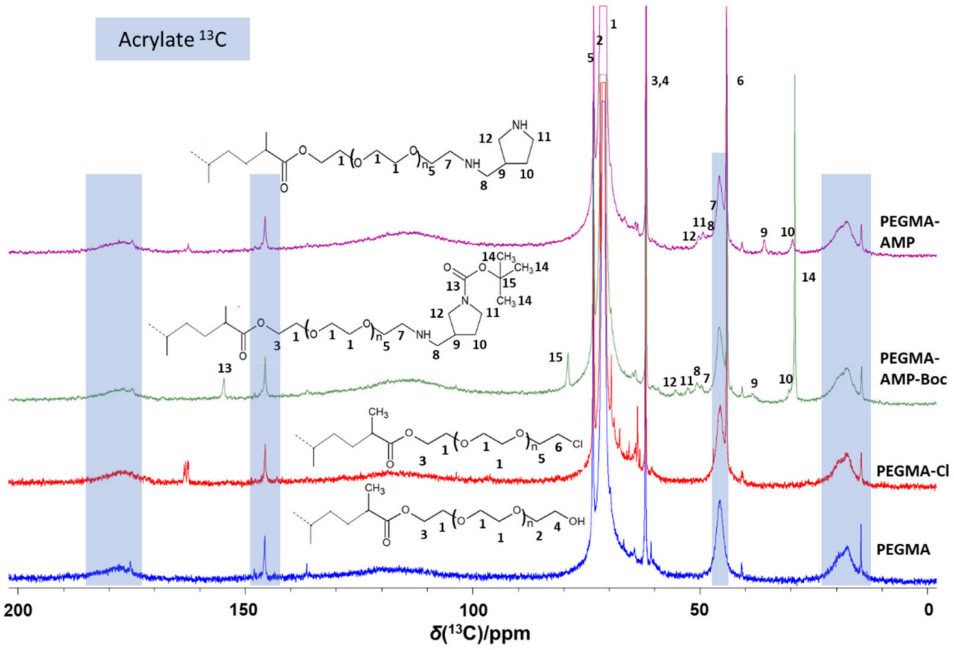

Figure A6. ^{13}C NMR spectra of (from bottom to top) the PEGMA support, the chlorine-functionalized PEGMA-Cl, the protected amine-functionalized PEGMA-AMP-Boc-3 and the aminated PEGMA-AMP-3. The spectrum is scaled vertically to magnify the diamine resonances.

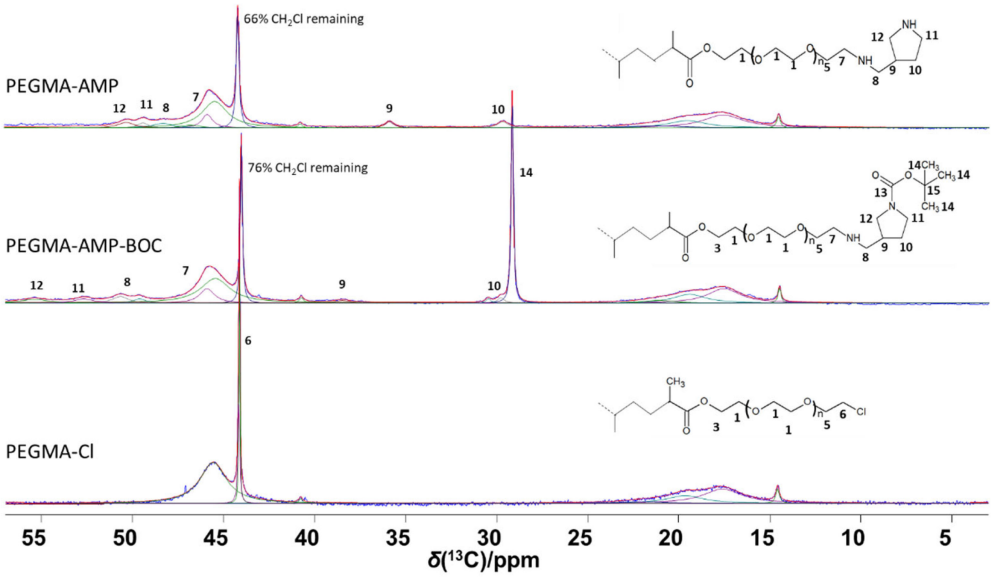

Figure A7. Spectral decomposition of ^{13}C NMR spectra of (from bottom to top) the chlorine-functionalized PEGMA-Cl, the protected amine-functionalized PEGMA-AMP-Boc-3 and the aminated PEGMA-AMP-3 in the chemical shift region 3–57 ppm.

Appendix D. Selectivity Profiles

Aldol condensations typically yield two main products (see Scheme 2). In the aldol reaction, the so-called aldol product (a β-hydroxy aldehyde or β-hydroxy ketone) is formed as the result of the coupling of the two reactants [1]. Dehydration of this aldol yields the so-called enone product (α,β-unsaturated carbonyl compound) [1].

In the aldol condensation of 4-nitrobenzaldehyde with acetone over PEGMA-AMP as catalyst in aqueous environment, the aldol product is formed as the main product, with a selectivity amounting to 97.7 ± 0.6%. The enone product is the secondary product, with a selectivity amounting to 2.3 ± 0.6%. As presented in Figure A8, initially only the aldol product is formed. Soon, however, the system evolves towards the aforementioned distribution and from 15% conversion onwards, the aldol product and enone product are in equilibrium while the conversion remains increasing till > 85%.

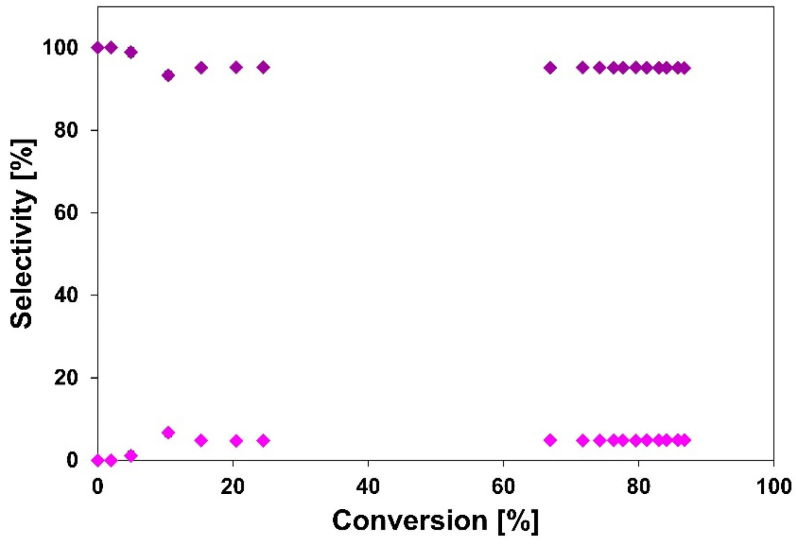

Figure A8. Selectivity profile of the aldol product (◆) and enone product (◆) in the aldol condensation of 4-nitrobenzaldehyde with acetone at 55 °C in a 50/50 vol% mixture of acetone/water with PEGMA-AMP-3 as catalyst. Error bars represent the 95% confidence interval.

In the aldol condensation of 4-nitrobenzaldehyde with acetone in a 50/50 vol% mixture of acetone/*n*-hexane, a similar trend was observed, though the selectivity for the aldol product was lower (91 ± 1.7%) and for the enone product was higher (9.2 ± 1.7%). This can be attributed to the low water concentration in the reaction environment. Nonetheless, it should be pointed out that due to the high affinity of water for the PEGMA support, the scarce water that was present (formed in the dehydration step) will preferentially remain absorbed by the catalyst instead of dissolving into the bulk liquid. The catalyst can get enriched with water, which will then affect the equilibrium between aldol and enone.

Hence, the dehydration of the aldol product forming the enone product and one water molecule should be regarded as reversible, at least from a thermodynamic point of view, not necessarily from a kinetic point of view, and the reaction environment can significantly affect the equilibrium between aldol and enone.

References

1. Biesemans, B.; De Clercq, J.; Stevens, C.V.; Thybaut, J.W.; Lauwaert, J. Recent advances in amine catalyzed aldol condensations. *Catal. Rev.* **2022**, 1–83. [CrossRef]
2. List, B.; Lerner, R.A.; Barbas, C.F. Proline-Catalyzed Direct Asymmetric Aldol Reactions. *J. Am. Chem. Soc.* **2000**, *122*, 2395–2396. [CrossRef]
3. Machajewski, T.D.; Wong, C.-H. The Catalytic Asymmetric Aldol Reaction. *Angew. Chem. Int. Ed.* **2000**, *39*, 1352–1375. [CrossRef]
4. Hajos, Z.G.; Parrish, D.R. Asymmetric Synthesis of Organic Compounds. U.S. Patent and Trademark Office US3975440A, 8 August 1971.
5. Eder, U.; Sauer, G.; Wiechert, R. New Type of Asymmetric Cyclization to Optically Active Steroid CD Partial Structures. *Angew. Chem. Int. Ed.* **1971**, *10*, 496–497. [CrossRef]
6. Hajos, Z.G.; Parrish, D.R. Asymmetric synthesis of bicyclic intermediates of natural product chemistry. *J. Org. Chem.* **1974**, *39*, 1615–1621. [CrossRef]
7. List, B. Proline-catalyzed asymmetric reactions. *Tetrahedron* **2002**, *58*, 5573–5590. [CrossRef]
8. Emma, M.G.; Tamburrini, A.; Martinelli, A.; Lombardo, M.; Quintavalla, A.; Trombini, C. A Simple and Efficient Protocol for Proline-Catalysed Asymmetric Aldol Reaction. *Catalysts* **2020**, *10*, 649. [CrossRef]
9. Melchiorre, P.; Marigo, M.; Carlone, A.; Bartoli, G. Asymmetric Aminocatalysis—Gold Rush in Organic Chemistry. *Angew. Chem. Int. Ed.* **2008**, *47*, 6138–6171. [CrossRef]
10. The Nobel Prize in Chemistry. 2021. Available online: https://www.nobelprize.org/prizes/chemistry/2021/summary/ (accessed on 21 October 2021).
11. Sakthivel, K.; Notz, W.; Bui, T.; Barbas, C.F. Amino Acid Catalyzed Direct Asymmetric Aldol Reactions: A Bioorganic Approach to Catalytic Asymmetric Carbon−Carbon Bond-Forming Reactions. *J. Am. Chem. Soc.* **2001**, *123*, 5260–5267. [CrossRef]
12. Brunelli, N.A.; Venkatasubbaiah, K.; Jones, C.W. Cooperative Catalysis with Acid–Base Bifunctional Mesoporous Silica: Impact of Grafting and Co-condensation Synthesis Methods on Material Structure and Catalytic Properties. *Chem. Mater.* **2012**, *24*, 2433–2442. [CrossRef]
13. Lauwaert, J.; De Canck, E.; Esquivel, D.; Thybaut, J.W.; Van Der Voort, P.; Marin, G.B. Silanol-Assisted Aldol Condensation on Aminated Silica: Understanding the Arrangement of Functional Groups. *ChemCatChem* **2014**, *6*, 255–264. [CrossRef]
14. Lauwaert, J.; Moschetta, E.G.; Van Der Voort, P.; Thybaut, J.W.; Jones, C.W.; Marin, G.B. Spatial arrangement and acid strength effects on acid–base cooperatively catalyzed aldol condensation on aminosilica materials. *J. Catal.* **2015**, *325*, 19–25. [CrossRef]
15. Lauwaert, J.; De Canck, E.; Esquivel, D.; Van Der Voort, P.; Thybaut, J.W.; Marin, G.B. Effects of amine structure and base strength on acid–base cooperative aldol condensation. *Catal. Today* **2015**, *246*, 35–45. [CrossRef]
16. Collier, V.E.; Ellebracht, N.C.; Lindy, G.I.; Moschetta, E.G.; Jones, C.W. Kinetic and Mechanistic Examination of Acid–Base Bifunctional Aminosilica Catalysts in Aldol and Nitroaldol Condensations. *ACS Catal.* **2016**, *6*, 460–468. [CrossRef]
17. Hoyt, C.B.; Lee, L.-C.; Cohen, A.E.; Weck, M.; Jones, C.W. Bifunctional Polymer Architectures for Cooperative Catalysis: Tunable Acid–Base Polymers for Aldol Condensation. *ChemCatChem* **2017**, *9*, 137–143. [CrossRef]
18. Kandel, K.; Althaus, S.M.; Peeraphatdit, C.; Kobayashi, T.; Trewyn, B.G.; Pruski, M.; Slowing, I.I. Solvent-Induced Reversal of Activities between Two Closely Related Heterogeneous Catalysts in the Aldol Reaction. *ACS Catal.* **2013**, *3*, 265–271. [CrossRef]
19. De Vylder, A.; Lauwaert, J.; Esquivel, D.; Poelman, D.; De Clercq, J.; Van Der Voort, P.; Thybaut, J.W. The role of water in the reusability of aminated silica catalysts for aldol reactions. *J. Catal.* **2018**, *361*, 51–61. [CrossRef]
20. Z Andrade, K.C.; Alves, M.L. Environmentally Benign Solvents in Organic Synthesis: Current Topics. *Curr. Org. Chem.* **2005**, *9*, 195–218. [CrossRef]
21. Ranu, B.C.; Saha, A.; Dey, R. Using more environmentally friendly solvents and benign catalysts in performing conventional organic reactions. *Curr. Opin. Drug Discov. Dev.* **2010**, *13*, 658–668.
22. Jing, Y.; Guo, Y.; Xia, Q.; Liu, X.; Wang, Y. Catalytic Production of Value-Added Chemicals and Liquid Fuels from Lignocellulosic Biomass. *Chem* **2019**, *5*, 2520–2546. [CrossRef]

23. De Vylder, A.; Lauwaert, J.; Van Auwenis, S.; De Clercq, J.; Thybaut, J.W. Catalyst Stability Assessment in a Lab-Scale Liquid-Solid $(LS)^2$ Plug-Flow Reactor. *Catalysts* **2019**, *9*, 755. [CrossRef]
24. Font, D.; Jimeno, C.; Pericàs, M.A. Polystyrene-Supported Hydroxyproline: An Insoluble, Recyclable Organocatalyst for the Asymmetric Aldol Reaction in Water. *Org. Lett.* **2006**, *8*, 4653–4655. [CrossRef] [PubMed]
25. Salam, N.; Mondal, P.; Mondal, J.; Roy, A.S.; Bhaumik, A.; Islam, S.M. Highly efficient base catalysis and sulfide oxidation reactions over new functionalized mesoporous polymers. *RSC Adv.* **2012**, *2*, 6464–6477. [CrossRef]
26. Xiao, J.; Li, G.-w.; Zhang, W.-q. Aldol reactions catalyzed by proline functionalized polyacrylonitrile fiber. *Chem. Res. Chin. Univ.* **2013**, *29*, 256–262. [CrossRef]
27. Zhu, H.; Zhang, C.; Ma, N.; Tao, M.; Zhang, W. Surface wettability modification of amine-functionalized polyacrylonitrile fiber to enhance heterogeneous catalytic performance for aldol reaction in water. *Appl. Catal. A Gen.* **2020**, *608*, 117842. [CrossRef]
28. De Vylder, A.; Lauwaert, J.; De Clercq, J.; Van Der Voort, P.; Jones, C.W.; Thybaut, J.W. Aminated poly(ethylene glycol) methacrylate resins as stable heterogeneous catalysts for the aldol reaction in water. *J. Catal.* **2020**, *381*, 540–546. [CrossRef]
29. Schmiegel, C.J.; Baier, R.; Kuckling, D. Direct Asymmetric Aldol Reaction in Continuous Flow Using Gel-Bound Organocatalysts. *Eur. J. Org. Chem.* **2021**, *2021*, 2578–2586. [CrossRef]
30. Xiao, W.; Wang, Z.; Yang, J.; Chen, T.; Yi, C.; Xu, Z. Engineering of polystyrene-supported acid–base catalysts for aldol condensation in water. *New J. Chem.* **2022**, *46*, 12318–12323. [CrossRef]
31. Shajahan, R.; Sarang, R.; Saithalavi, A. Polymer Supported Proline-Based Organocatalysts in Asymmetric Aldol Reactions: A Review. *Curr. Organocatal.* **2022**, *9*, 124–146. [CrossRef]
32. Tuncel, A. Suspension polymerization of poly(ethylene glycol) methacrylate: A route for swellable spherical gel beads with controlled hydrophilicity and functionality. *Colloid Polym. Sci.* **2000**, *278*, 1126–1138. [CrossRef]
33. De Vylder, A.; Lauwaert, J.; Sabbe, M.K.; Reyniers, M.-F.; De Clercq, J.; Van Der Voort, P.; Thybaut, J.W. Rational design of nucleophilic amine sites via computational probing of steric and electronic effects. *Catal. Today* **2019**, *334*, 96–103. [CrossRef]
34. Singh, S.; Chimni, S.S. Pyrrolidine catalyzed diastereoselective direct aldol reaction in water: A green approach. *Indian J. Chem.* **2013**, *52B*, 1202–1209.
35. Harris, J.M.; Hundley, N.H.; Shannon, T.G.; Struck, E.C. Polyethylene glycols as soluble, recoverable, phase-transfer catalysts. *J. Org. Chem.* **1982**, *47*, 4789–4791. [CrossRef]
36. Gravert, D.J.; Janda, K.D. Organic Synthesis on Soluble Polymer Supports: Liquid-Phase Methodologies. *Chem. Rev.* **1997**, *97*, 489–510. [CrossRef]
37. Kandel, K.; Althaus, S.M.; Peeraphatdit, C.; Kobayashi, T.; Trewyn, B.G.; Pruski, M.; Slowing, I.I. Substrate inhibition in the heterogeneous catalyzed aldol condensation: A mechanistic study of supported organocatalysts. *J. Catal.* **2012**, *291*, 63–68. [CrossRef]
38. Lauwaert, J.; Ouwehand, J.; De Clercq, J.; Cool, P.; Van Der Voort, P.; Thybaut, J.W. Tuning component enrichment in amino acid functionalized (organo)silicas. *Catal. Commun.* **2017**, *88*, 85–89. [CrossRef]
39. De Vylder, A.; Lauwaert, J.; Sabbe, M.K.; Reyniers, M.-F.; De Clercq, J.; Van Der Voort, P.; Thybaut, J.W. A comprehensive model for the role of water and silanols in the amine catalyzed aldol reaction. *Chem. Eng. J.* **2021**, *404*, 127070. [CrossRef]
40. Bartók, M. Advances in Immobilized Organocatalysts for the Heterogeneous Asymmetric Direct Aldol Reactions. *Catal. Rev.* **2015**, *57*, 192–255. [CrossRef]
41. Chen, J.-Y.; Pineault, H.; Brunelli, N.A. Quantifying the fraction and activity of catalytic sites at different surface densities of aminosilanes in SBA-15 for the aldol reaction and condensation. *J. Catal.* **2022**, *413*, 1048–1055. [CrossRef]
42. Córdova, A.; Notz, W.; Barbas Iii, C.F. Direct organocatalytic aldol reactions in buffered aqueous media. *Chem. Commun.* **2002**, 3024–3025. [CrossRef]
43. Nyberg, A.I.; Usano, A.; Pihko, P.M. Proline-Catalyzed Ketone-Aldehyde Aldol Reactions are Accelerated by Water. *Synlett* **2004**, *2004*, 1891–1896. [CrossRef]
44. Córdova, A.; Zou, W.; Ibrahem, I.; Reyes, E.; Engqvist, M.; Liao, W.-W. Acyclic amino acid-catalyzed direct asymmetric aldol reactions: Alanine, the simplest stereoselective organocatalyst. *Chem. Commun.* **2005**, 3586–3588. [CrossRef] [PubMed]
45. Doyagüez, E.G.; Calderón, F.; Sánchez, F.; Fernández-Mayoralas, A. Asymmetric Aldol Reaction Catalyzed by a Heterogenized Proline on a Mesoporous Support. The Role of the Nature of Solvents. *J. Org. Chem.* **2007**, *72*, 9353–9356. [CrossRef] [PubMed]
46. Vachan, B.S.; Karuppasamy, M.; Vinoth, P.; Sridharan, V.; Menéndez, J.C. Chapter 6—Stereoselective organic synthesis in water: Organocatalysis by proline and its derivatives. In *Green Sustainable Process for Chemical and Environmental Engineering and Science*; Inamuddin, Boddula, R., Asiri, A.M., Eds.; Elsevier: Amsterdam, The Netherlands, 2020; pp. 191–229. [CrossRef]
47. Christensen, J.J.; Izatt, R.M.; Wrathall, D.P.; Hansen, L.D. Thermodynamics of proton ionization in dilute aqueous solution. Part XI. pK, ΔH°, and ΔS° values for proton ionization from protonated amines at 25°. *J. Chem. Soc. A Inorg. Phys. Theor.* **1969**, 1212–1223. [CrossRef]
48. Singappuli-Arachchige, D.; Kobayashi, T.; Wang, Z.; Burkhow, S.J.; Smith, E.A.; Pruski, M.; Slowing, I.I. Interfacial Control of Catalytic Activity in the Aldol Condensation: Combining the Effects of Hydrophobic Environments and Water. *ACS Catal.* **2019**, *9*, 5574–5582. [CrossRef]
49. Lauwaert, J.; Van de Steene, E.; Vermeir, P.; De Clercq, J.; Thybaut, J.W. Critical Assessment of the Thermodynamics in Acidic Resin-Catalyzed Esterifications. *Ind. Eng. Chem. Res.* **2020**, *59*, 22079–22091. [CrossRef]

50. Di Carmine, G.; Forster, L.; Wang, S.; Parlett, C.; Carlone, A.; D'Agostino, C. NMR relaxation time measurements of solvent effects in an organocatalysed asymmetric aldol reaction over silica SBA-15 supported proline. *React. Chem. Eng.* **2022**, *7*, 269–274. [CrossRef]
51. Brunelli, N.A.; Didas, S.A.; Venkatasubbaiah, K.; Jones, C.W. Tuning Cooperativity by Controlling the Linker Length of Silica-Supported Amines in Catalysis and CO2 Capture. *J. Am. Chem. Soc.* **2012**, *134*, 13950–13953. [CrossRef]
52. Brunelli, N.A.; Jones, C.W. Tuning acid–base cooperativity to create next generation silica-supported organocatalysts. *J. Catal.* **2013**, *308*, 60–72. [CrossRef]
53. Han, G.; Tamaki, M.; Hruby, V.J. Fast, efficient and selective deprotection of the tert-butoxycarbonyl (Boc) group using HCl/dioxane (4 m). *J. Pept. Res.* **2001**, *58*, 338–341. [CrossRef]
54. Huybrechts, W.; Lauwaert, J.; De Vylder, A.; Mertens, M.; Mali, G.; Thybaut, J.W.; Van Der Voort, P.; Cool, P. Synthesis of L-serine modified benzene bridged periodic mesoporous organosilica and its catalytic performance towards aldol condensations. *Microporous Mesoporous Mater.* **2017**, *251*, 1–8. [CrossRef]
55. Houlleberghs, M.; Hoffmann, A.; Dom, D.; Kirschhock, C.E.A.; Taulelle, F.; Martens, J.A.; Breynaert, E. Absolute Quantification of Water in Microporous Solids with 1H Magic Angle Spinning NMR and Standard Addition. *Anal. Chem.* **2017**, *89*, 6940–6943. [CrossRef] [PubMed]
56. Radhakrishnan, S.; Colaux, H.; Chandran, C.V.; Dom, D.; Verheyden, L.; Taulelle, F.; Martens, J.; Breynaert, E. Trace Level Detection and Quantification of Crystalline Silica in an Amorphous Silica Matrix with Natural Abundance 29Si NMR. *Anal. Chem.* **2020**, *92*, 13004–13009. [CrossRef] [PubMed]
57. Massiot, D.; Fayon, F.; Capron, M.; King, I.; Le Calvé, S.; Alonso, B.; Durand, J.-O.; Bujoli, B.; Gan, Z.; Hoatson, G. Modelling one- and two-dimensional solid-state NMR spectra. *Magn. Reson. Chem.* **2002**, *40*, 70–76. [CrossRef]